ELSEVIER

Solid State Ionics 82 (1995) 67–73

SOLID STATE IONICS

In situ deposition and XPS characterization of lithium based solid glass electrolyte/vanadia interfaces: Observation of lithium migration

D.A. Hensley, S.H. Garofalini

Department of Ceramics and Interfacial Molecular Science Laboratory, Institute of Engineered Materials, Rutgers, The State University of New Jersey, Piscataway, NJ 08855-0909, USA

Received 22 June 1995; accepted for publication 31 July 1995

Abstract

In situ X-ray Photoelectron Spectroscopy (XPS) was used to examine the interfaces formed by reactive sputter deposition of vanadia onto several lithium based solid glass electrolytes. It has been found that lithium migration to the vanadia/vacuum interface can occur during deposition and that the presence of lithium can influence the oxygen uptake during the reactive sputtering process. The lithium migration is driven by an electric field present due to the plasma; it is shown that the migration can be influenced by the deposition conditions.

Keywords: Interfacial lithium migration; Lithium phosphate; Lithium phosphorus oxynitride; Vanadium pentoxide; XPS

1. Introduction

The current interest in thin film ionic devices such as microbatteries and electrochromic windows has driven researchers to investigate a number of lithium ion conducting and mixed electron/ion conducting glasses for use as electrolytes, anodes and cathodes in these devices [1]. A number of reports of working prototype ionic devices have also been reported in the literature [2–4]. Failures of some of these prototypes have suggested the need for better understanding of the numerous interfaces involved in these devices [5,6]. The focus of this work has been to investigate the electrolyte/cathode interface found in solid state inorganic ionic conducting devices. In previous work it has been shown that both structural and compositional changes can occur at the lithium anode/electrolyte interface, and that such changes can be observed by surface analytical techniques such as XPS [7]. Others have shown similar results using these techniques to examine the lithium metal/silica glass interface [8].

The materials chosen for this study, vanadium pentoxide as a cathode, and lithium phosphorus oxynitride, lithium phosphate, and lithium borate glasses as electrolytes, have previously been the subject of ionic conductivity studies and have been used in devices reported in the literature [9–12]. For example, a promising microbattery utilizing a lithium phosphorus oxynitride electrolyte and a vanadium pentoxide cathode has been reported by Bates et al. [3]. In that work, deposition of the lithium phosphorus oxynitride was done by magnetron sputtering of Li_3PO_4 using N_2 as the sputter gas, leading to incorporation of nitrogen into the glass network. The V_2O_5 deposition was done by reactive magnetron

0167-2738/95/$09.50 © 1995 Elsevier Science B.V. All rights reserved
SSDI 0167-2738(95)00191-3

sputtering using a V target and an argon/oxygen mix as the sputtering gas.

The goal of this work was to investigate the interfaces present in such devices by examining the initial stages of vanadia deposition onto several lithium based glass electrolytes. By using in situ XPS, the composition in the surface region near the interface could be followed for a series of vanadia depositions, providing information about the interface region as it is formed. Film deposition in an attached deposition chamber allowed for in situ analysis of all of the interfaces involved. By doing this type of analysis, the complications of atmospheric contamination, such as the formation of a lithium carbonate surface layer, are avoided. This in situ technique has been used previously to identify surface diffusion and the formation of reaction layers at the interfaces of lithium containing compounds [7,8].

2. Experimental

2.1. Target fabrication

The lithium phosphate, lithium phosphorus oxynitride, and vanadium oxide films examined in these experiments were deposited by RF magnetron sputtering using a 1 inch diameter UHV compatible magnetron sputter system from K. Lesker (Clairton, PA). The lithium phosphate and lithium phosphorus oxynitride films were deposited using lithium phosphate targets made by pressing Li_3PO_4 powder (Aldrich Chemical Co.) into disks, and sintering at 900°C. Theoretical densities of 85% were typically observed. The targets were then ground down to the appropriate size in order to fit into the magnetron. The vandaium pentoxide films were deposited using a 99.95% pure vanadium target obtained commercially (K. Lesker Co.).

The lithium borate films were deposited by thermal evaporation of crystalline $LiBO_2$ from a tungsten basket filament, and the procedure has been described previously in detail [12].

2.2. Rf sputter deposition

All films were deposited onto either native oxide covered *p*-type silicon wafer substrates or microscope slide glass. The depositions were done in a two stage UHV chamber with a base pressure of 10^{-9} Torr after baking. This system has been described previously [12]. While this background pressure was maintained in the spectrometer side of the chamber, the deposition side was opened after bake out in order to change sputter targets and insert new substrates. As a result, background pressures of 5×10^{-8} Torr were typical in the deposition chamber. Sputter deposition was done using a 1 inch diameter magnetron source from K. Lesker. The source was powered by a RF power supply and impedance matching circuit from Applied Energy. During sputter deposition, the working gas was admitted to the chamber from the gas manifold, and the pressure was controlled by a MKS mass flow controller. Source to sample distance was 5 cm.

For deposition of the lithium phosphate films, argon was used as the working gas and a pressure of 5 millitorr was maintained. The RF power was 30 W and deposition rates of 1 Å per minute were observed For the lithium phosphorus oxynitride films, the working gas was N_2 at a pressure of 6 millitorr, and the power was 30 W. The vanadium oxide films were deposited by reactive sputtering of a vanadium target using a working gas with a composition of 16% O_2 and 84% Ar, at a pressure of 5 millitorr and a power of 60 W. Despite the higher power, the deposition rate of these films was slower, typically only 0.5 Å per minute. Deposition thicknesses were montitored by a quartz crystal deposition monitor located 2 cm from the sample. Calibration of the deposition monitor was done by interferometry measurements of a V_2O_5 film deposited directly onto a silicon wafer substrate. XPS was used for an additional calibration by examining the attenuation of the Si2p peak as various amounts of V_2O_5 were deposited onto the silicon wafer.

2.3. XPS

After deposition of a film, the sample was moved into the analysis chamber and normal incidence XPS spectra were obtained. Survey scans of the entire energy spectrum and higher resolution scans over the peaks of interest were recorded. The spectrometer used was a Kratos XSAM-800, operated in the Fixed Analyser Transmission (also called Constant Anal-

yser Energy) mode. The X-rays were produced by the Mg anode with a power of 250 W. After the appropriate spectra were recorded, the sample was moved back to the connected deposition chamber for additional thin film deposition.

2.4. Interface analysis

The technique used to examine the electrolyte/cathode interface was to deposit a thickness of one of the lithium electrolytes mentioned above, followed by XPS survey and elemental scans. While the sample was kept at UHV in the analysis chamber, the deposition chamber was opened and the vanadium target was installed. After a suitable pump-down time, the sample was moved into the deposition chamber for vanadia deposition. After 25 to 50 Å of vanadia were deposited onto the lithium electrolyte material, the deposition was stopped and additional XPS survey and elemental spectra were recorded. This procedure was repeated in order to build up hundreds of Ångströms of vanadia onto the lithium electrolyte surface. In this way, the interface at various stages of development could be observed without the added complications of atmospheric contamination or sputtering artifacts common to destructive depth profiling techniques.

3. Results

3.1. Lithium electrolytes

The freshly deposited lithium phosphate films examined in these experiments typically had a stoichiometry of $LiPO_3$, despite the fact that the target composition was Li_3PO_4. This composition is based on integration of the areas under the O1s, P2p, and Li1s XPS peaks, divided by their respective sensitivity factors. The O1s peak was separated into bridging and non-bridging components, with a ratio of 70% to 30%, as expected for a phosphate glass with this composition.

The lithium phosphorus oxynitride had a composition similar to the lithium phosphate, with the addition of a small amount of nitrogen incorporated into the glass structure. The composition measured by XPS was $LiPO_{3.1}N_{0.14}$, similar to that reported by Bates et al. [3].

The evaporated lithium borate films had a composition close to that of $LiBO_2$ and have been investigated in detail previously [12].

3.2. Vanadium pentoxide

A 200 Å thick vanadia film was deposited directly onto a silicon wafer substrate by reactive sputtering. In order to check the deposition cleanliness and composition, XPS spectra were recorded. The film had a composition of 72% oxygen and 28% vanadium, as expected for V_2O_5. The binding energy difference between the O1s peak and the $V2p_{3/2}$ peak was 12.9 eV, which is consistant with values found in the literature [13].

3.3. Vanadium pentoxide on the lithium based glass electrolytes

For the case of the vanadia/lithium phosphate structure grown on the silicon wafer substrates, a series of 50 Å depositions totaling typically up to 600 Å of vanadia were grown on films of lithium phosphate with thicknesses of 50, 100, 120, 200, 300, 375, 500, and 750 Å. The surface composition as a function of vanadia thickness on the 300 Å lithium phosphate as measured by XPS is shown in Fig. 1. It is clear that although the phosphate peak is strongly attenuated by the deposition of the vanadia,

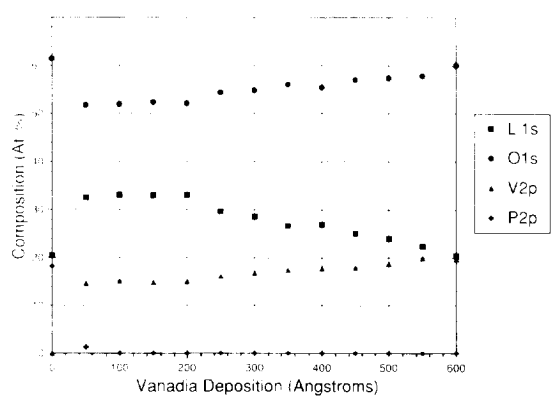

Fig. 1. XPS surface composition for reactively sputtered vanadium oxide grown on a 300 Å thick layer of lithium phosphate on a silicon wafer. Although the phosphorus peak is quickly attenuated after the first deposition, a strong lithium is still observed after the deposition of 600 Å of vanadia, indicating migration of the lithium to the vanadia/vacuum interface.

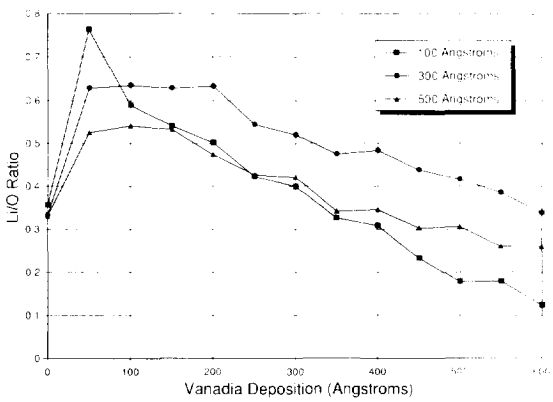

Fig. 2. A plot of the Li/O ratio as a function of vanadia deposition for films grown on three different thicknesses of lithium phosphate (100, 300, and 500 Å) on a silicon substrate. The trend seen here, in which higher lithium content at 50 Å of vanadia was observed for the thinner films was observed consistently.

the lithium peak is not attenuated, indicating a migration of lithium out of the phosphate and into the growing vanadia layer. It is also clear that the vanadium to oxygen ratio is not that of V_2O_5 until several hundred Ångströms beyond the interface. For some of these runs, the binding energy difference between the O1s peak and the $V2p_{3/2}$ was observed to decrease slightly from 12.9 to 12.7 eV for the first

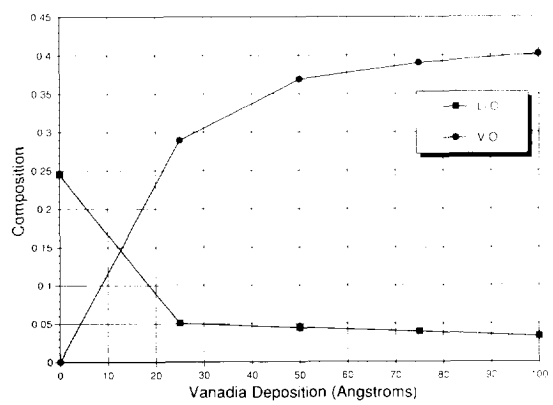

Fig. 3. Li/O and V/O ratios plotted as a function of vanadia deposition for vanadia grown on 130 Å lithium phosphate film on a 2 mm thick glass substrate. In this case, the lithium content drops off quickly and the vanadium to oxygen ratio rapidly approaches 0.4, the value for vanadium pentoxide.

100–200 Å, then shift back to 12.9 eV. No evidence of an increase in this difference, which would be expected for a reduction of the vanadium, was ever observed.

In Fig. 2, the lithium to oxygen ratio for three runs which differ only in the thickness of the lithium phosphate film thickness are plotted, and the trends seen in these three were seen in all of the runs. For vanadium on the 100 Å thick lithium phosphate film, the lithium concentration jumps up to a high value, then quickly decreases as the deposition thickness increases. For the 300 Å film, the value initially increases, although not as high as for the first case, then falls off, but more gradually than for the first case. For the 500 Å lithium phosphate film case, again the lithium concentration grows, although not as high as in the previous cases, but then falls off even more gradually. Despite the fact that all of the deposition parameters were held constant, these trends were seen consistantly.

Similar results were observed for vanadia grown on lithium phosphorus oxynitride and lithium borate glasses as well. For both of these materials, like the lithium phosphate, in situ XPS scans clearly revealed high concentrations of lithium present at the vanadia/vacuum interface. This suggests that this lithium migration is possible from any lithium ion conducting material if exposed to vanadia deposition conditions similar to those described here. Again, here the initial ion conducting films were grown on a substrate of *p*-type doped silicon wafer. For the case of the lithium phosphorus oxynitride, the nitrogen peak was not observed after the initial vanadia deposition indicating that no nitrogen diffusion into the vanadia occurs. Similarly, for vanadia on the lithium borate, no evidence of boron diffusion was observed.

It is important to note that although the plots in Figs. 1 and 2 resemble depth profiles, they should not be viewed as such. If the area under the lithium curve in Fig. 1 is measured and used to calculate a total amount of lithium in the vanadia, it is found that more lithium is present in the vanadia than was originally present in the lithium phosphate layer. Since XPS samples only the top 50 Å, it must be concluded that the lithium content is higher in the surface region, and that the lithium is migrating to the vanadia/vacuum interface and depleting previously analyzed regions.

Instead of *p*-type Si as the substrate upon which the electrolyte/cathode thin films were deposited, similar depositions were done on 2 mm thick glass substrates. In this case, different results were observed. After deposition of 130 Å of lithium phosphate from the same target used previously, XPS scans revealed a composition of 16% Li, 20% P and 64% O. Subsequently, vanadia was deposited onto this lithium phosphate film, and the resultant XPS scans showed no evidence of lithium migration into the vanadia layer. This result is shown in Fig. 3, in which the lithium to oxygen and vanadium to oxygen ratios are plotted as a function of the amount of vanadia deposited. After just 25 Å of vanadia deposition, the Li and P peaks are both strongly attenuated, and by 50 Å, the V to O ratio is 0.37, very close to the value of 0.4 expected for V_2O_5.

In summary, the lithium electrolyte/vanadia thin film structures grown on silicon wafer substrates showed strong evidence of migration of the lithium into the vanadia and evidence that the presence of the lithium influenced the vanadium to oxygen ratio during film formation. Evidence of this was not observed for similar thin film structures grown on a glass substrate.

4. Discussion

Although the experiments described in the preceeding section were done under similar conditions, the difference in the substrates did influence the conditions during deposition. It is known that electrically isolated surfaces in a plasma will develop a negative potential of a few Volts, often called the "floating" potential [14]. In the current experimental configuration, a voltage of −1.3 V was measured at the sample holder during deposition. Such a potential on the surface would give rise to an electric field between the film surface and the nearest ground. Although the silicon wafer substrate was not grounded, it was attached to the grounded sample holder by either double sided, non-conducting tape or UHV compatible ceramic epoxy. In either case, although the wafer is not grounded, the fact that the doped wafer is conducting leads to a polarization of the free charges in the wafer, effectively forming two capacitors acting in series. This is diagrammed in Fig. 4. Since the thin film structure is thinner than the adhesive used to mount the substrate on the sample holder, and capacitance is inversely proportional to the separation distance of the electrodes, the polarization of the charges has the effect of concentrating most of the voltage drop across the thin film structure, and, therefore, applying a strong electric field to the thin film structure. The electric field drives the mobile lithium ions out of the lithium phosphate and into the growing vanadia layer. Since the field strength is inversely proportional to the thickness of the vanadia/lithium phosphate film structure, this makes the results seen in Fig. 2 easily understood. For the 100 Å thick lithium phosphate layer, the field is the strongest, forcing more lithium to move to the vanadia. As the thickness of vanadia increases, the field strength is reduced, and less lithium is forced to the vanadia/vacuum interface. Similarly, for the cases of the 300 Å and 500 Å thick lithium phosphate films, the initial depositions of vanadia are onto thicker lithium phosphate films, which have correspondingly weaker electric fields. For these cases, as observed, less lithium is driven to the vanadia/vacuum interface, and as a result, less lithium is detected by the XPS scans.

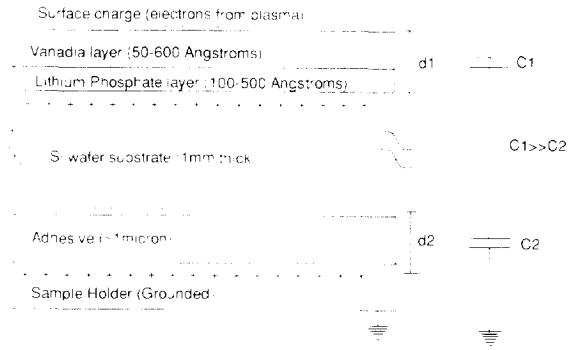

Fig. 4. Diagram depicting charges during deposition of vanadia onto the doped silicon wafer. Due to free charges in the silicon, two capacitors are present, and an electric field is concentrated across the thin film structure. This field drives the lithium ions toward the vanadia/vacuum interface and affects oxygen uptake during deposition.

A second observation from Fig. 2 is that at higher vanadia thicknesses, the Li/O ratio drops off much faster for the 100 Å case. This was also observed in similar experiments of vanadia deposited onto 50 and 120 Å thick lithium phosphate films, suggesting

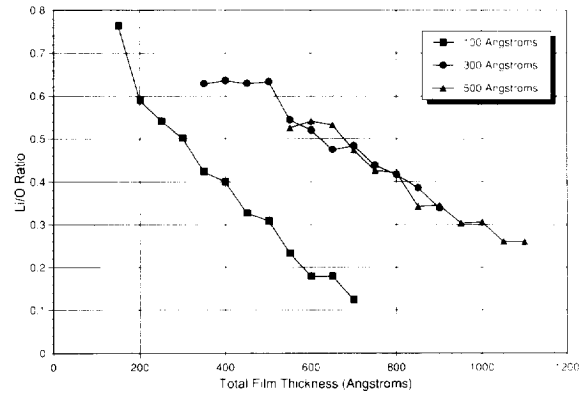

Fig. 5. A plot of the Li/O ratio as a function of total film thickness for the same lithium phosphate films shown in Fig. 2. The data from vanadia on the 300 and 500 Å thick lithium phosphate films are very similar at a given total film thickness; at equivalent thicknesses, the electric field across the film should be similar. For the 100 Å case, the Li/O ratio falls off more quickly due to the insufficient lithium supply from the thinner film.

that these thinner films do not supply as much lithium to the vanadia as do the thicker films. Thus, although the field is stronger for the thinner films at low vanadia thicknesses, only a limited amount of lithium is available to migrate into the vanadia. For the thicker initial lithium phosphate films, more lithium is available, and higher lithium concentrations are measured as the vanadia thickness increases. In Fig. 5, the same data shown in Fig. 2 is plotted, not as a function of vanadia thickness, but as a function of total film thickness. In this case, the electric field driving the lithium should be roughly equivalent at any given point for all of the films. It can be seen that although the Li/O ratio for the 100 Å film drops off very quickly, the data for the 300 and 500 Å thick films are very similar, suggesting that for these thicker lithium phosphate films, sufficient lithium is available to saturate the vanadia/vacuum interface region at a given electric field strength.

As an additional test for this idea, the case of the vanadia/lithium phosphate structure grown onto a 2 mm thick glass substrate was done. In this case the electric field is distributed over the thin film structure and the thickness of the glass, having the effect of weakening the electric field by an estimated 4 orders of magnitude, simply because of the increased thickness and the lack of free carriers in the glass. In this case, as mentioned in the results section, no migration of the lithium into the vanadia was observed and the vanadia was observed to have the expected composition for V_2O_5 within 100 Å of the interface. More evidence of this electric field effect was observed in the composition of the newly deposited lithium phosphate films. Compositions of the lithium phosphate films deposited onto the silicon wafer were consistantly 19% Li, 18% P and 63% O; however on the glass substrate it was measured to be 16% Li, 20% P and 64% O. A subsequent deposition of lithium phosphate onto a silicon wafer substrate produced film with composition similar to that observed previously on a wafer, indicating that target aging was not the cause of this compositional change. Again, the presence of an electric field during deposition would force lithium ions to the negatively charged surface, affecting the compositional measurement by XPS.

The formation of this vanadia/lithium phosphate layer onto these two differing substrates represents the limiting cases for which this interface structure can be formed. In a typical ionic device, both conducting and non-conducting layers are present around the cathode/electrolyte interface, such as a lithiated anode layer in an electrochromic or a carbon/lithium anode in a microbattery. It is conceivable that such a conducting layer could act in a manner similar to the silicon wafer in these experiments, allowing a strong electric field to be concentrated across an interface structure. As seen here, such a field is capable of driving the lithium to the cathode/vacuum interface during deposition. The presence of excess cations at this interface can affect the formation of subsequent layers, by influencing the oxygen uptake during reactive sputtering, even several hundred Ångströms away from the interface.

5. Conclusions

These experiments have investigated interface formed by reactive sputtering of vanadia onto lithium phosphate, lithium phosphorus oxynitride, and lithium borate under various conditions. It has been observed that electric fields present during deposi-

tion can strongly influence the composition of the cathode material. Lithium migration to the cathode/vacuum interface can strongly influence the oxygen uptake during reactive sputtering, as far as 600 Å away from the interface. For the case of weakened electric fields, no evidence of lithium migration is observed, suggesting that this behavior can be controlled.

Acknowledgements

We would like to acknowledge support from DOE, OBES, Chemical Sciences, DE-FG02-93ER 14385 and use of the facilities in the Center for Ceramic Research at Rutgers University.

References

[1] See for example: B.V.R. Chowdari and S. Radhakrishna, eds. in: Solid State Ionic Devices, World Scientific Singapore, 1988).

[2] K. Kanehori, K. Matsumo, K. Miyauchi and T. Kudo, Solid State Ionics 9/10 (1983) 1445.

[3] J.B. Bates, N.J. Dudney, G.R. Gruzalski, R.A. Zuhr, A. Chowdury, C.F. Luck and J.D. Robertson, J. Power Sources 43/44 (1993) 103.

[4] S.D. Jones, J.R. Akridge and F.K. Shokobi, Solid State Ionics 69 (1994) 357.

[5] H. Ohtsuka, S. Okada and J. Yamaki, Solid State Ionics 40/41 (1990) 964.

[6] K. Wiesener, W. Schneider, D. Ilic and E. Stegel, J Power Sources 20 (1987) 157.

[7] D.A. Hensley and S.H. Garofalini, Appl. Surface Sci. 81 (1994) 331.

[8] B.L. Maschoff, K.R. Zavadil and N.R. Armstrong, Appl Surface Sci. 27 (1986) 285.

[9] N.J. Dudney, J.B. Bates, R.A. Zuhr and C.F. Luck, Solid State Ionics 53–56 (1992) 655.

[10] J.B. Bates, N.J. Dudney, G.R. Gruzalski, R.A. Zuhr, A. Choudhury, C.F. Luck and J.D. Robertson, Solid State Ionics 53–56 (1992) 647.

[11] P. Dzwonkonski, C. Julien and M. Balkanski, Appl. Surface Sci. 33/34 (1988) 838.

[12] M. Eddrief, P. Dzwonkonski, J.Y. Emery, C. Julien and M. Balkanski, Solid State Ionics 45 (1990) 77.

[13] C.D. Wagner, W.M. Riggs, L.E. Davis and J.F. Moulder, Handbook of X-ray Photoelectron Spectroscopy (Perkin-Elmer, Eden Prarie, MN 1979).

[14] J.L. Vossen and W. Kern, eds., in: Thin Film Processes II (Academic Press, Boston, 1991).